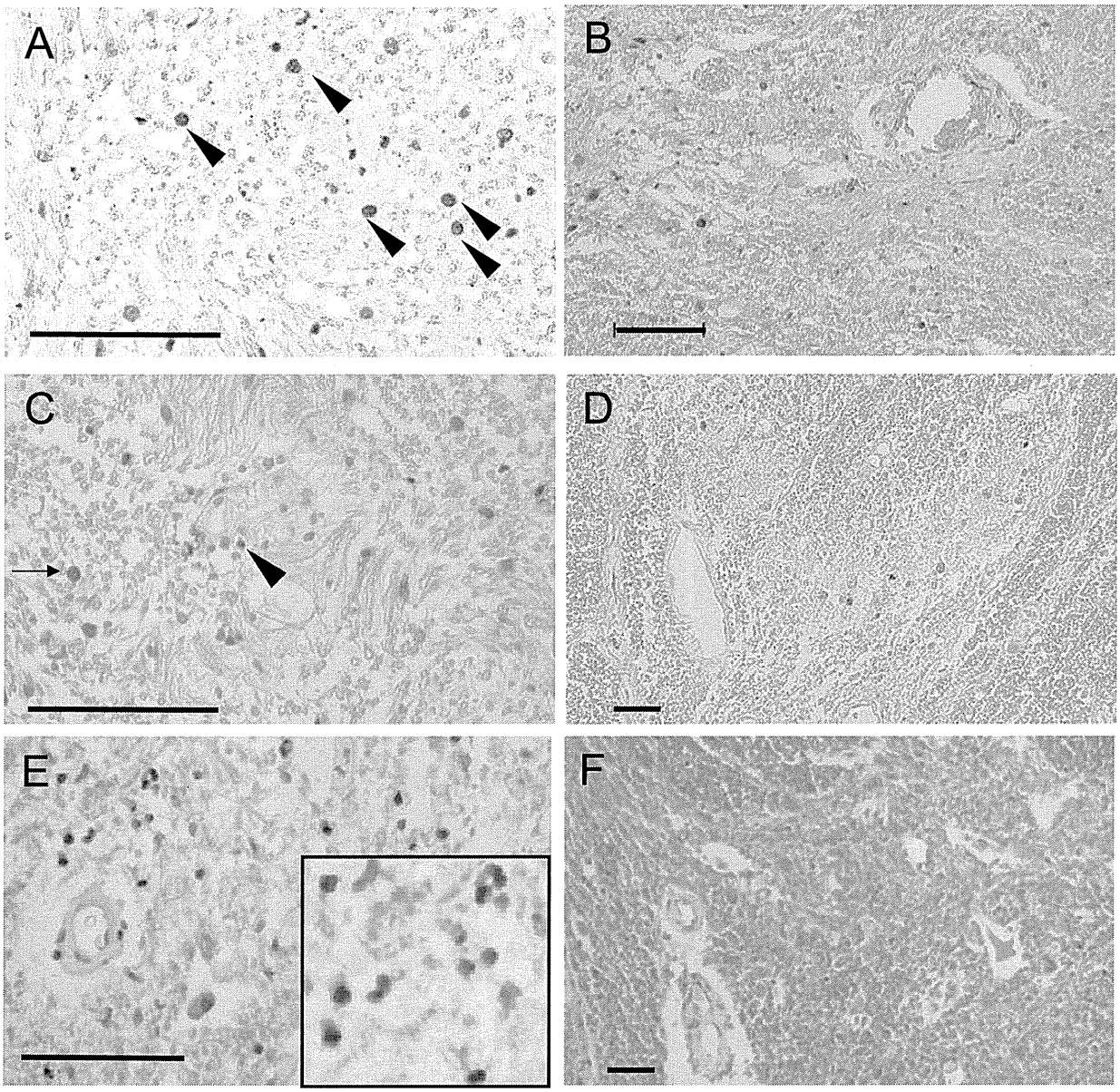

FIGURE 6. Detection of apoptotic cells in the CNS. **(A)** Some small cells are apoptotic (DAB; brown, arrowheads) detected by anti–active caspase-3 antibody (Ab). **(B–D)** TdT-mediated dUTP nick end labeling assay. **(B)** A number of apoptotic cells (DAB; brown) are detected in the spinal cord of a patient with HTLV-1–associated myelopathy/tropical spastic paraparesis (Patient 8624). **(C)** Some infiltrating small cells around a small vessel (arrowhead) and some relatively large cells in the parenchyma (arrow) are apoptotic. **(D)** The apoptotic cells are barely detectable in the control spinal cord from an HTLV-1–seronegative patient with hepatoma. **(E, F)** Anti-single-stranded DNA antibody staining. **(E)** Numerous apoptotic cells (AEC; red) are detected in the spinal cord (Patient 8624). A higher magnification picture in the inset shows apoptotic cells. **(F)** Apoptotic cells are barely detectable in the control patient spinal cord. Scale bar = 100 μm.

HTLV-1–infected cells could express viral antigens anywhere in the body of the infected individuals (14, 32), the expression of HTLV-1 proteins in vivo has remained elusive so far.

In this study, we succeeded in detecting HTLV-1 proteins in the CD4-positive T cells infiltrating the CNS. This is consistent with our previous reports in which HTLV-1–infected cells were determined to be CD4-positive lymphocytes in the CNS by in situ hybridization for HTLV-1 mRNA and in situ polymerase chain reaction for HTLV-1 DNA (33, 34). The infiltrating HTLV-1–infected CD4-positive cells may easily express the viral antigens in the CNS, which in turn facilitates the accumulation of HTLV-1–specific CTLs.

Human T-lymphotropic virus type-1 infection causes several organ-specific inflammatory diseases including HAM/TSP (2, 3). Previous reports demonstrating that HTLV-1 proviral loads are high in affected organs such as the muscles, lungs, and CNS suggest that HTLV-1–infected cells accumulate in the organs (13, 35). The pathogenesis model in which both

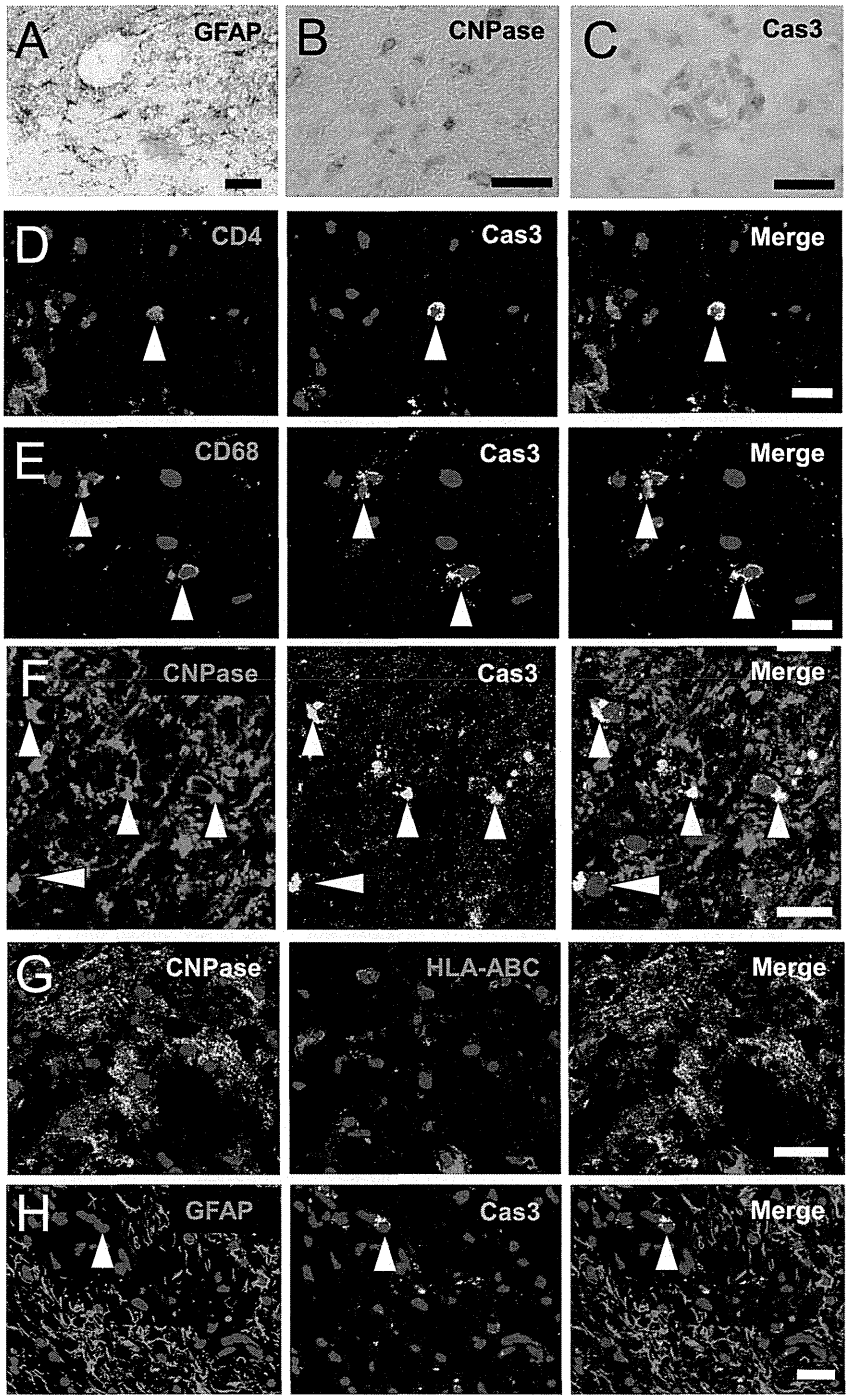

FIGURE 7. Cell identification of apoptotic cells. **(A–C)** Astrocytes **(A)**, oligodendrocytes **(B)**, and apoptotic cells **(C)** were stained with anti–glial fibrillary acidic protein (GFAP) antibody (Ab), anti–2′,3′-cyclic-nucleotide 3′-phosphodiesterase (CNPase) monoclonal antibody (mAb), or anti–active caspase-3 Ab, respectively, in the spinal cord of Patient 8624. Nuclei were counterstained with hematoxylin. **(D–F, H)** Double staining revealed that a CD4-positive cell (red, **D**), a CD68-positive cell (red, **E**), and some oligodendrocytes (red, **F**), but no astrocytes (red, **H**), were apoptotic (green) (arrowheads) in the spinal cord of Patient 8624. **(G)** Double staining with anti-CNPase mAb (green) and anti–HLA-ABC mAb (red) revealed that no oligodendrocyte expresses HLA-ABC. There is no double-positive signal (yellow) in the merged image. White bars indicate 20 μm. Cas3, active caspase-3.

HTLV-1–infected CD4-positive T cells and the virus-specific CD8-positive CTLs infiltrate the organs from the peripheral blood followed by bystander tissue damage may explain why HTLV-1 infection can cause several chronic inflammatory diseases in various organs. Further studies are needed to determine whether the similar immunopathologic model can be applied to HTLV-1–associated inflammatory diseases in other organs.

ACKNOWLEDGMENT

The authors thank Ms. T. Inoue for her excellent technical assistance.

REFERENCES

1. Uchiyama T, Yodoi J, Sagawa K, et al. Adult T-cell leukemia: Clinical and hematologic features of 16 cases. Blood 1977;50:481–92
2. Gessain A, Barin F, Vernant JC, et al. Antibodies to human T-lymphotropic virus type-I in patients with tropical spastic paraparesis. Lancet 1985;2: 407–10
3. Osame M, Usuku K, Izumo S, et al. HTLV-I–associated myelopathy: A new clinical entity. Lancet 1986;1:1031–32
4. Osame M, Matsumoto M, Usuku K, et al. Chronic progressive myelopathy associated with elevated antibodies to human T-lymphotropic virus type I and adult T-cell leukemialike cells. Ann Neurol 1987;21:117–22
5. Nakao K, Ohba N, Isashiki M, et al. Pigmentary retinal degeneration in patients with HTLV-I–associated myelopathy. Jap J Ophthalmol 1989; 33:383–91
6. Nishioka K, Maruyama I, Sato K, et al. Chronic inflammatory arthropathy associated with HTLV-I. Lancet 1989;1:441
7. Morgan OS, Rodgers-Johnson P, Mora C, et al. HTLV-1 and polymyositis in Jamaica. Lancet 1989;2:1184–87
8. Higuchi I, Nerenberg M, Yoshimine K, et al. Failure to detect HTLV-I by in situ hybridization in the biopsied muscles of viral carriers with polymyositis. Muscle Nerve 1992;15:43–47
9. Ozden S, Gessain A, Gout O, et al. Sporadic inclusion body myositis in a patient with human T cell leukemia virus type 1–associated myelopathy. Clin Infect Dis 2001;32:510–14
10. Matsuura E, Umehara F, Nose H, et al. Inclusion body myositis associated with human T-lymphotropic virus–type I infection: Eleven patients from an endemic area in Japan. J Neuropathol Exp Neurol 2008;67:41–49
11. Sugimoto M, Nakashima H, Watanabe S, et al. T-lymphocyte alveolitis in HTLV-I–associated myelopathy. Lancet 1987;2:1220
12. Nagai M, Usuku K, Matsumoto W, et al. Analysis of HTLV-I proviral load in 202 HAM/TSP patients and 243 asymptomatic HTLV-I carriers: High proviral load strongly predisposes to HAM/TSP. J Neurovirol 1998;4:586–93
13. Hayashi D, Kubota R, Takenouchi N, et al. Accumulation of human T-lymphotropic virus type I (HTLV-I)–infected cells in the cerebrospinal fluid during the exacerbation of HTLV-I–associated myelopathy. J Neurovirol 2008;14:459–63
14. Jacobson S, Gupta A, Mattson D, et al. Immunological studies in tropical spastic paraparesis. Ann Neurol 1990;27:149–56
15. Kubota R, Furukawa Y, Izumo S, et al. Degenerate specificity of HTLV-1–specific $CD8^+$ T cells during viral replication in patients with HTLV-1–associated myelopathy (HAM/TSP). Blood 2003;101:3074–81
16. Biddison WE, Kubota R, Kawanishi T, et al. Human T cell leukemia virus type I (HTLV-I)–specific $CD8^+$ CTL clones from patients with HTLV-I–associated neurologic disease secrete proinflammatory cytokines, chemokines, and matrix metalloproteinase. J Immunol 1997;159:2018–25
17. Kubota R, Kawanishi T, Matsubara H, et al. Demonstration of human T lymphotropic virus type I (HTLV-I) tax–specific $CD8^+$ lymphocytes directly in peripheral blood of HTLV-I–associated myelopathy/tropical spastic paraparesis patients by intracellular cytokine detection. J Immunol 1998;161:482–88
18. Greten TF, Slansky JE, Kubota R, et al. Direct visualization of antigen-specific T cells: HTLV-1 Tax11-19–specific CD8(+) T cells are activated in peripheral blood and accumulate in cerebrospinal fluid from HAM/TSP patients. Proc Natl Acad Sci USA 1998;95:7568–73
19. Levin MC, Lehky TJ, Flerlage AN, et al. Immunologic analysis of a spinal cord-biopsy specimen from a patient with human T-cell lymphotropic virus type I–associated neurologic disease. N Engl J Med 1997;336:839–45
20. Skinner PJ, Daniels MA, Schmidt CS, et al. Cutting edge: In situ tetramer staining of antigen-specific T cells in tissues. J Immunol 2000; 165:613–17
21. Ijichi S, Izumo S, Eiraku N, et al. An autoaggressive process against bystander tissues in HTLV-I–infected individuals: A possible pathomechanism of HAM/TSP. Med Hypoth 1993;41:542–47
22. Kozako T, Arima N, Toji S, et al. Reduced frequency, diversity, and function of human T cell leukemia virus type 1–specific $CD8^+$ T cell in adult T cell leukemia patients. J Immunol 2006;177:5718–26
23. Yashiki S, Fujiyoshi T, Arima N, et al. HLA-A*26, HLA-B*4002, HLA-B*4006, and HLA-B*4801 alleles predispose to adult T cell leukemia: The limited recognition of HTLV type 1 tax peptide anchor motifs and epitopes to generate anti-HTLV type 1 tax CD8(+) cytotoxic T lymphocytes. AIDS Res Hum Retroviruses 2001;17:1047–61
24. Bunce M, O'Neill CM, Barnardo MC, et al. Phototyping: Comprehensive DNA typing for HLA-A, B, C, DRB1, DRB3, DRB4, DRB5 & DQB1 by PCR with 144 primer mixes utilizing sequence-specific primers (PCR-SSP). Tissue Antigens 1995;46:355–67
25. Lee B, Tanaka Y, Tozawa H. Monoclonal antibody defining tax protein of human T-cell leukemia virus type-I. Tohoku J Exp Med 1989;157:1–11
26. Hayashi D, Kubota R, Takenouchi N, et al. Reduced Foxp3 expression with increased cytomegalovirus-specific CTL in HTLV-I–associated myelopathy. J Neuroimmunol 2008;200:115–24
27. Haring JS, Pewe LL, Perlman S. Bystander CD8 T cell–mediated demyelination after viral infection of the central nervous system. J Immunol 2002;169:1550–55
28. Fung-Leung WP, Kundig TM, Zinkernagel RM, et al. Immune response against lymphocytic choriomeningitis virus infection in mice without CD8 expression. J Exp Med 1991;174:1425–29
29. Marcondes MC, Burudi EM, Huitron-Resendiz S, et al. Highly activated CD8(+) T cells in the brain correlate with early central nervous system dysfunction in simian immunodeficiency virus infection. J Immunol 2001;167:5429–38
30. Kannagi M, Matsushita S, Shida H, et al. Cytotoxic T cell response and expression of the target antigen in HTLV-I infection. Leukemia 1994; 1(Suppl 8):S54–59
31. Hanon E, Asquith RE, Taylor GP, et al. High frequency of viral protein expression in human T cell lymphotropic virus type 1–infected peripheral blood mononuclear cells. AIDS Res Hum Retroviruses 2000; 16:1711–15
32. Nagasato K, Nakamura T, Ohishi K, et al. Active production of anti-human T-lymphotropic virus type I (HTLV-I) IgM antibody in HTLV-I–associated myelopathy. J Neuroimmunol 1991;32:105–9
33. Moritoyo T, Reinhart TA, Moritoyo H, et al. Human T-lymphotropic virus type I–associated myelopathy and tax gene expression in $CD4^+$ T lymphocytes. Ann Neurol 1996;40:84–90
34. Matsuoka E, Takenouchi N, Hashimoto K, et al. Perivascular T cells are infected with HTLV-I in the spinal cord lesions with HTLV-I–associated myelopathy/tropical spastic paraparesis: Double staining of immunohistochemistry and polymerase chain reaction in situ hybridization. Acta Neuropathol 1998;96:340–46
35. Seki M, Higashiyama Y, Mizokami A, et al. Up-regulation of human T lymphotropic virus type 1 (HTLV-1) tax/rex mRNA in infected lung tissues. Clin Exp Immunol 2000;120:488–98

INTERNAL MEDICINE

□ CASE REPORT □

A Family with Distal Hereditary Motor Neuropathy and a K141Q Mutation of Small Heat Shock Protein *HSPB1*

Kengo Maeda[1], Ryo Idehara[1], Akihiro Hashiguchi[2] and Hiroshi Takashima[2]

Abstract

We herein describe a Japanese family with distal hereditary motor neuropathy carrying a K141Q mutation of small heat shock protein *HSPB1*. Two patients among them had late onset disease (older than 50 years). The muscles of the distal legs were weak and atrophic. Sensory and autonomic dysfunction were not seen. Even eight years after onset, one patient could still walk without support. A nerve conduction study revealed axonal degeneration of the motor nerves of the legs. A heterozygous K141Q mutation was detected in the affected patients. The late onset and mild clinical phenotype might reflect the mild biochemical alteration of HSP27 induced by the K141Q mutation.

Key words: Charcot-Marie-Tooth disease, distal hereditary motor neuropathy, heat shock protein

(Intern Med 53: 1655-1658, 2014)
(DOI: 10.2169/internalmedicine.53.2843)

Introduction

Mutations of several genes are known to cause distal hereditary motor neuropathy (dHMN). There is often an overlap with Charcot-Marie-Tooth disease (CMT2) and the juvenile form of amyotrophic lateral sclerosis. Heat shock protein (HSP) 27 is one of the causative proteins resulting in dHMN or CMT2F. Its clinical phenotypes differ based on the *HSPB1* mutations (1). In Japan, only three families with dHMN and *HSPB1* mutations have been reported so far (2-4). We herein report another family with dHMN with a mutation in this gene.

Case Reports

Case 1 (the proband)

A 69-year-old man presented with gait disturbance which had appeared one year earlier. He did not have numbness in his feet. Before the onset, he had been exercising at a gym near his house. He had not been exposed to any toxic organic solvent or heavy metals. There were some individuals showing similar symptoms in his family.

During the initial examination, the patient was alert, and there were no abnormal finding for his cranial nerves. Muscular atrophy was obvious in his legs, and pes cavus was observed (Fig. 1A). The muscle strength was decreased to 4/4 in the anterior tibial muscles. The strength of the other muscles was normal. Sensations of light touch, pain, temperature, vibration, and position were normal. The tendon reflexes were symmetrical and decreased in all four limbs. No pathological reflex was evoked. The patient's coordination was normal. He could not stand on his heels. He did not have any autonomic symptoms, such as orthostatic hypotension or urinary incontinence. The complete blood cell count was normal. The erythrocyte sedimentation ratio was 13/33 mm (one hour/two hours). The parameters of liver function and renal function were within the normal limits. The serum level of creatine kinase was mildly elevated, to 488 IU/L. The levels of fasting blood glucose, electrolytes, and lipids were normal. Anti-nuclear antibody, proteinase 3-anti-neutrophil cytoplasmic antibody (PR3-ANCA), and myeloperoxidase (MPO)-ANCA, and the levels of vitamin B 1, B12 and folic acid were normal.

The cell count of the cerebrospinal fluid (CSF) was 2/3 mm^3. The levels of protein and glucose in the CSF were 46 mg/dL and 64 mg/dL, respectively. A nerve conduction

[1]Department of Neurology, National Hospital Organization Higashi-ohmi General Medical Center, Japan and [2]Department of Neurology and Geriatrics, Kagoshima University Graduate School of Medical and Dental Sciences, Japan
Received for publication March 7, 2014; Accepted for publication March 31, 2014
Correspondence to Dr. Kengo Maeda, maeda-kengo@shiga-hosp.jp

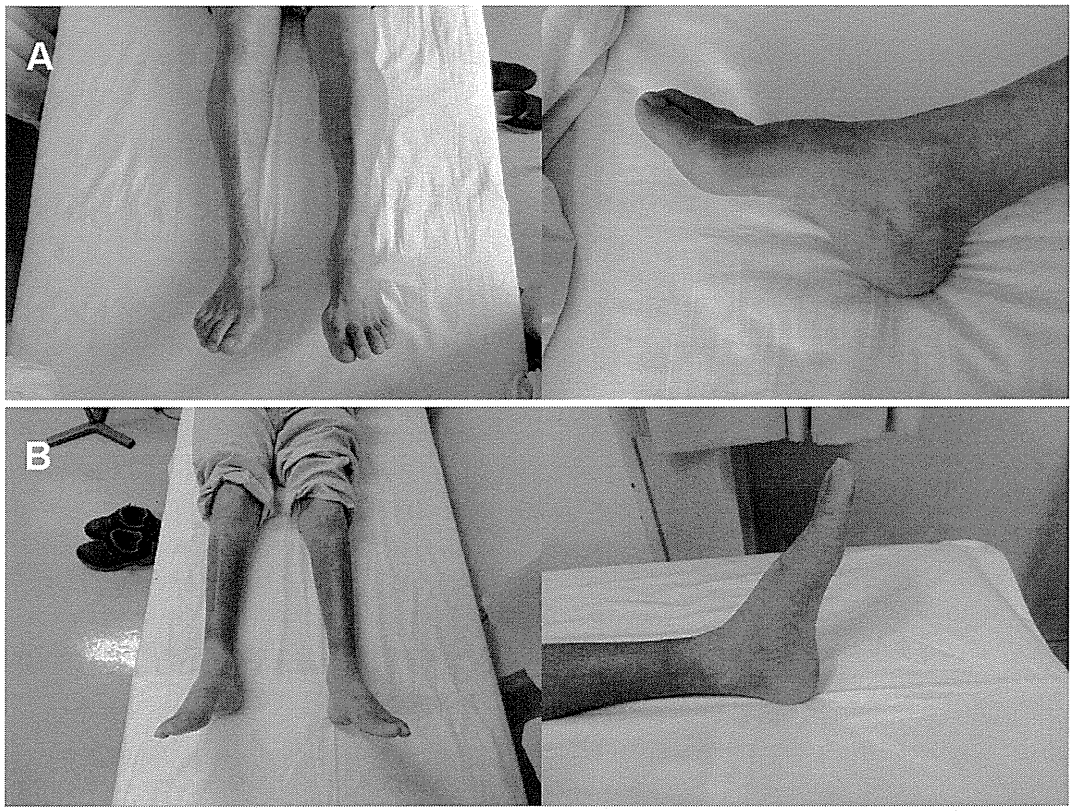

Figure 1. Photographs of the patients' legs (left) and feet (right). A: Case 1, B: Case 2

Table. The Results of the Nerve Conduction Study of Case 1

Nerve	Motor						Sensory					
	DL (ms)		CV (m/s)		CMAP(mV)		DL (ms)		CV (m/s)		SNAP (μV)	
	R	L	R	L	R	L	R	L	R	L	R	L
Median	5.5	4.8	53	52	7.3	6.7	3.3	2.9	60	62	24	33
Ulnar	2.7	2.5	61	61	4.7	7.3	2.3	2.2	66	78	25	26
Tibial	6.9	6.4	40	34	0.4	1.1						
Sural							3.3	3.0	42	47	4.2	14

DL: distal latency, CV: conduction velocity, CMAP: compound muscle action potential, SNAP: sensory nerve action potential, R: right, L: left

study (Table) revealed a decreased amplitude of the compound muscle action potentials in the tibial nerves. The amplitudes of the other motor nerves were relatively spared. The amplitude of the sensory nerve action potential was not decreased, except for the right sural nerve. The conduction velocities were not decreased in either the motor or sensory nerves. He refused to undergo a sural nerve biopsy.

Case 2 (the son of the proband's cousin)

The second patient was sixty years old at the time of our examination. He had experienced difficulty walking for eight years. His grandmother had also experienced difficulty walking. The patient's calf was atrophic and pes cavus was also found (Fig. 1B). The muscle strength was 1/1 at the anterior tibial muscles and 2/2 at the gastrocnemius muscles. The strength of the other muscles was normal. He did not have any sensory symptoms, such as numbness. The sensations of light touch and temperature were normal, but the vibration sensation was slightly decreased. All tendon reflexes were decreased. No pathological reflex was evoked. He could walk by himself without any support.

Other family members (Fig. 2A)

Three cousins of the proband had similar symptoms. One of them had previously been examined at another hospital. He had undergone sural nerve biopsy and was diagnosed with axonal type CMT, but had not undergone a genetic diagnosis. Although the surviving patients had some level of walking disability, their activity of daily life was relatively preserved. The disease onset was after age fifty in all of the patients. Although we asked the family members to undergo re-examination of their neurological condition, they rejected our proposal.

Gene analysis of the proband and his family (Fig. 2B)

Genomic DNA was extracted from the peripheral blood leukocytes of the patients using the Gentra Puregene Blood

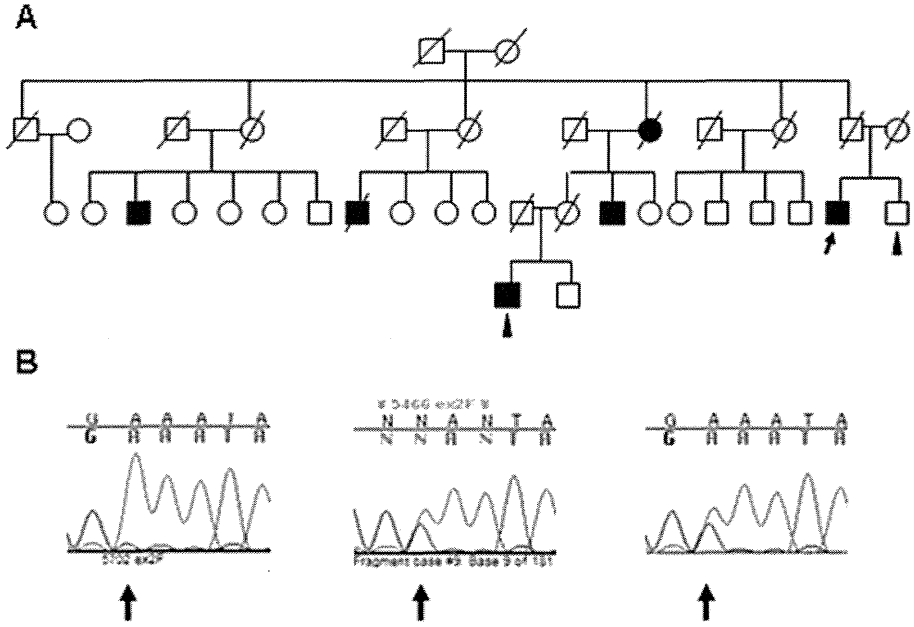

Figure 2. **The pedigree of the family with the heat shock protein 27 (HSP27) c.412A>C mutation (A). The arrow indicates Case 1 (the proband). The arrowheads indicate subjects who underwent a genetic analysis. Open circles (women) and squares (men) denote unaffected individuals, and filled symbols denote affected family members. Symbols with a strike through them indicate deceased family members. The electropherograms for the brother of Case 1 (left), Case 1 (middle), and Case 2 (right) (B). The arrows indicate nucleotide 421 in *HSPB1*.**

Kit (Qiagen, Duesseldorf, Germany). A panel of sixty genes, including 40 known CMT disease-causing genes and 20 candidate genes were screened (AARS, ANKG, APTX, ARHGEF10, CARS, CNTF, CNTN2/TAG1, DARS, DHH, DNM2, EGR2, EPRS, FARSA, FARSB, FGD4, FIG4, GAN, GARS, GDAP1, GJB1, HARS, HK1, HOXD10, HSPB1, HSPB8, IARS, KARS, KCC3, LARS, LITAF, LMNA, MARS, MED25, MFN2, MPZ, MTMR2, NARS, NDRG1, NEFL, PEPD, PMP22, PRPS1, PRX, QARS, RAB7, RARS, SARS, SBF2, SCN8A, SETX, SH3TC2, SOX10, TARS, TDP1, TRPV4, TTR, VARS, WARS and, YARS). Using the Primer 3 program, we designed 861 oligonucleotide primers covering the entire coding exons and exon-intron junctions, with an amplicon length of 350-500 base pairs. Briefly, all fragments were amplified by multiplex polymerase chain reaction (PCR) (Qiagen Multiplex PCR Kit; Qiagen) and then were mixed to build the amplicon DNA library. As an initial input, 50 ng of the DNA library was fragmented and tagged simultaneously with the Nextera transposome, then multiple index 1 (i7) and index 2 (i5), as well as common adapters (P5 and P7, respectively) were ligated. After small DNA fragments (shorter than 300 bp) were removed using the AMPure PCR purification system (Agencourt Bioscience, Beverly, USA), the library was adjusted to a working concentration of 2 nM. The target resequence analysis was performed using a next-generation sequencer (MiSeq®, Illumina, San Diego, USA). After cluster generation through a bridge PCR, paired-end sequencing (150×2) was performed on a flow cells; clusters were imaged using light emitting diode (LED) and filter combinations specific to each of the four fluorescently-labeled dideoxynucleotides. After base-calling, filtering, and quality scoring, fastq files were generated. Using the CLC Genomics Workbench 6 software program (CLC bio, Aarhus, Denmark), the output reads were aligned with the reference sequence, and thereafter the variants were called and annotated for the analysis.

To confirm the mutation revealed by next-generation sequencer, the proband and two members of the family underwent a genetic analysis by the Sanger method for direct sequencing. In the two affected individuals, we detected a heterozygous c.421A>C (p.K141Q) missense mutation in the *HSPB1* gene. The proband's younger brother, who was neurologically normal, did not have this mutation.

Discussion

This family is the fourth reported Japanese family with autosomal dominant dHMN with a *HSPB1* mutation. The K141Q mutation was first reported by Ikeda et al. (4). The ages of onset of their two cases were 47 years and in the fifties. Compared with these patients, the onset in our Case 1 occurred at an older age. In the first reported family with this mutation, severe dysfunction of the autonomic nervous system was reported. Unlike that family, our patients did not complain of orthostatic hypotension or neurogenic bladder. However, the dysautonomia in the first reported family could have been due to complicated diabetes mellitus. The sensory involvement was minimal or subclinical in our cases, as well as in the previously reported cases.

Since the first report of *HSPB1* mutation (5), 16 different autosomal dominant mutations and one autosomal recessive mutation have been reported in families with CMT2 and dHMN (6-12). HSP27 is one of a stress-induced chaperone protein and forms oligomers to maintain a misfolded protein in a refolding-competent state. The upregulation of HSP27 has been reported to be required for the survival of motor and sensory neurons injured by apoptotic stress (13). In fact, higher levels of serum HSP27 have been reported in diabetic patients with better nerve function (14). Individuals with mutations in the C-terminal domain of HSP27 show a more severe phenotype, with ages at onset as young as four and seven years (2).

The K141Q substitution is located in the α-crystallin domain of HSP27. The K141Q mutation does not dramatically affect the quaternary structure of HSP27. The chaperone-like activity associated with the K141Q mutation is only a little less than that of the wild-type protein. However, oligomers formed by proteins with the K141Q mutation are slightly larger and less stable than those formed of the wild type (15). The effects of the K141Q mutation on the aggregation of neurofilament light polypeptide or incorporation of neurofilament medium polypeptide into the cytoskeletal network remain to be clarified. Unlike patients with mutations in the C-terminal domain, patients with the K141Q mutation show late onset and a mild clinical phenotype, reflecting the minimal biochemical changes associated with this mutation (15).

The authors state that they have no Conflict of Interest (COI).

References

1. Rossor AM, Kalmar B, Greensmith L, Reilly MM. The distal hereditary motor neuropathies. J Neurol Neurosurg Psychiatry **83**: 6-14, 2012.
2. Kijima K, Numakura C, Goto T, et al. Small heat shock protein 27 mutation in a Japanese patient with distal hereditary motor neuropathy. J Hum Genet **50**: 473-476, 2005.
3. Nishibayashi M, Kokubun N, Nakamura A, Hirata K, Yamamoto M, Sobue G. Distal hereditary motor neuropathy type II with mutation in heat shock protein 27 gene. A case report. Rinsho Shinkeigaku (Clinical Neurology) **47**: 50-52, 2007 (in Japanese).
4. Ikeda Y, Abe A, Ishida C, Takahashi K, Hayasaka K, Yamada M. A clinical phenotype of distal hereditary motor neuronopathy type II with a novel *HSPB1* mutation. J Neurol Sci **277**: 9-12, 2009.
5. Evgrafov OV, Mersiyanova I, Irobi J, et al. Mutant small heat-shock protein 27 causes axonal Charcot-Marie-Tooth disease and distal hereditary motor neuropathy. Nature Gen **36**: 602-606, 2004.
6. Houlden H, Laura M, Wavrant-De Vriéze F, Blake J, Wood N, Reilly MM. Mutations in the HSP27 (*HSPB1*) gene cause dominant, recessive, and sporadic distal HMN/CMT type 2. Neurology **71**: 1660-1668, 2008.
7. Chung KW, Kim SB, Cho SY, et al. Distal hereditary motor neuropathy in Korean patients with a small heat shock protein 27 mutation. Exp Mol Med **40**: 304-312, 2008.
8. James PA, Rankin J, Talbot K. Asymmetrical late onset motor neuropathy associated with a novel mutation in the small heat shock protein *HSPB1* (HSP27). J Neurol Neurosurg Psychiatry **79**: 461-463, 2008.
9. Luigetti M, Fabrizi GM, Madia F, et al. A novel *HSPB1* mutation in an Italian patient with CMT2/dHMN phenotype. J Neurol Sci **298**: 114-117, 2010.
10. Mandich P, Grandis M, Varese A, et al. Severe neuropathy after diphtheria-tetanus-pertussis vaccination in a child carrying a novel frame-shift mutation in the small heat-shock protein 27 gene. J Child Neurol **25**: 107-109, 2010.
11. Solla P, Vannelli A, Bolino A, et al. Heat shock protein 27 R127W mutation: evidence of a continuum between axonal Charcot-Marie-Tooth and distal hereditary motor neuropathy. J Neurol Neurosurg Psychiatry **81**: 958-962, 2010.
12. Rossor AM, Davidson GL, Blake J, et al. A novel p.Glu175X premature stop mutation in the C-terminal end of HSP27 is a cause of CMT2. J Peripher Nerv Syst **17**: 201-205, 2012.
13. Benn SC, Perrelet D, Kato AC, Scholz J, Decosterd I, Mannion RJ. Hsp27 upregulation and phosphorylation is required for injured sensory and motor neuron survival. Neuron **36**: 45-56, 2004.
14. Pourhamidi K, Dahlin LB, Boman K, Rolandsson O. Heat shock protein 27 is associated with better nerve function and fewer signs of neuropathy. Diabetologia **54**: 3143-3149, 2011.
15. Nefedova VV, Datskevich PN, Sudnitsyna MV, Strelkov SV, Gusev NB. Physico-chemical properties of R140G and K141Q mutants of human small heat shock protein *HspB1* associated with hereditary peripheral neuropathies. Biochimie **95**: 1582-1592, 2013.

INTERNAL MEDICINE

□ CASE REPORT □

Partial Deficiency of Emerin Caused by a Splice Site Mutation in *EMD*

Junhui Yuan[1], Masahiro Ando[1], Itsuro Higuchi[1], Yusuke Sakiyama[1], Eiji Matsuura[1], Kumiko Michizono[1], Osamu Watanabe[1], Shinjiro Nagano[2], Yukie Inamori[1], Akihiro Hashiguchi[1], Yujiro Higuchi[1], Akiko Yoshimura[1] and Hiroshi Takashima[1]

Abstract

Emery-Dreifuss muscular dystrophy (EDMD) is caused by mutations in the *EMD* gene on the X chromosome, which codes for emerin, an inner nuclear membrane protein. Monoclonal antibodies against the N-terminus of emerin protein are used to screen for emerin deficiency in clinical practice. However, these tests may not accurately reflect the disease in some cases. We herein describe the identification of a splice site mutation in the *EMD* gene in a Japanese patient who suffered from complete atrioventricular conduction block, mild muscle weakness and joint contracture, and a persistently elevated serum creatine kinase level. We used multiple antibodies to confirm the presence of a novel truncating mutation in emerin without the transmembrane region and C-terminus in the skeletal muscle.

Key words: Emery-Dreifuss muscular dystrophy (EDMD), splice site mutation, emerin, immunohistochemical stain

(Intern Med 53: 1563-1568, 2014)
(DOI: 10.2169/internalmedicine.53.8922)

Introduction

Emery-Dreifuss muscular dystrophy (EDMD) is characterized by early contractures of the elbow, neck, and Achilles tendons; slowly progressive skeletal muscle wasting in the upper arms and lower legs (humeroperoneal); and cardiomyopathy associated with conduction defects (1). The most serious aspect of EDMD is cardiac involvement, which usually becomes evident as muscle weakness progresses, but it may occur before there is any significant skeletal muscle involvement. EDMD is caused by mutations in different genes; including those in the *EMD* gene, encoding emerin, and causing X-linked EDMD (2); mutations in the *LMNA* gene, which encodes lamins A and C, and causes autosomal dominant EDMD (3) and a very rare autosomal recessive EDMD (4).

Monoclonal antibodies against the N-terminus of emerin, including Novocastra™ Lyophilized Mouse Monoclonal Antibody Emerin (NCL-emerin), have been used to screen emerin deficiency in clinical practice. In general, previous studies only used one kind of antibody in western blot or immunocytochemistry tests to evaluate emerin expression. Most of the mutations (86%) affecting males result in a complete absence of emerin (5); however, the corresponding genotypes were different, indicating that pathological assessments using a single antibody could not accurately reflect patients' diverse genetic information.

We herein describe the case of a patient with typical complete atrioventricular conduction block along with mild muscle weakness and joint contracture. We identified a previously reported splice acceptor site mutation in *EMD*, but the original symptoms and clinical severity of our case are different from those of the previous patient with this mutation (6). Furthermore, immunohistochemistry using three antibodies against different emerin domains revealed a distinct partial deficiency of emerin in the nuclei of the skeletal muscle fibers.

[1]Department of Neurology and Geriatrics, Kagoshima University Graduate School of Medical and Dental Sciences, Japan and [2]Department of Cardiology, Imamura Bun-in Hospital, Japan
Received for publication September 5, 2012; Accepted for publication January 30, 2014
Correspondence to Dr. Hiroshi Takashima, thiroshi@m3.kufm.kagoshima-u.ac.jp

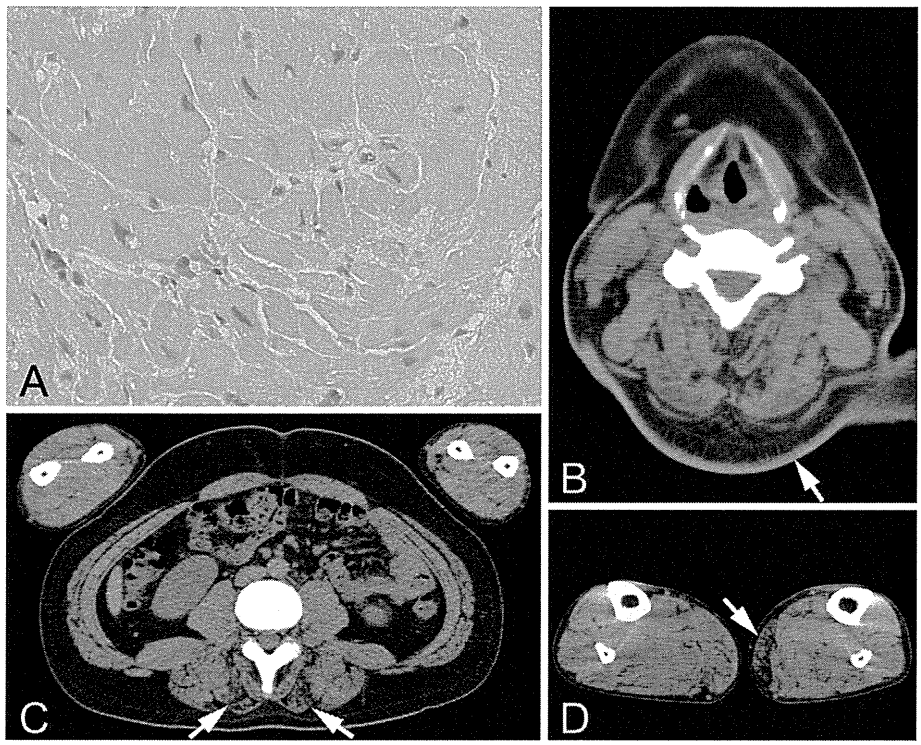

Figure 1. Cardiac pathology and CT findings of the paraspinal muscles and gastrocnemius. Hematoxylin and Eosin staining revealed mild myocardial interstitial fibrosis (×800) (A). A CT revealed low-density areas and atrophic changes (arrows) in the cervical and lumbar paraspinal muscles (B, C) and the left gastrocnemius (D).

Case Report

A 22-year-old male with normal growth and development was referred to our hospital with a complaint of chest discomfort at the age of 19 years. He had a complete atrioventricular conduction block (heart rate, 38/min), and his serum creatine kinase (CK) was elevated to 3,000 IU/mL (normal range 45-163 IU/mL). A chest X-ray and echocardiography (ECG) revealed no cardiomegaly. His symptoms gradually worsened, and symptoms of dizziness appeared due to bradycardia. The R-R interval of the ECG was extended to 9.2 s. Six months after the initial diagnosis, the patient was implanted with a permanent pacemaker. A sample of the left ventricular myocardium was obtained during cardiac catheterization, and histochemical staining revealed mild myocardial interstitial fibrosis without fiber disarray, fibril deposition, or myocardial injury (Fig. 1A). No abnormalities were detected in the respiratory function tests. Although he had suffered from diplopia and strabismus several years earlier, a neurological examination on admission showed normal ocular movement. His cognition, coordination, and facial muscle strength were also normal. The patient's neck flexion was slightly weak and was limited due to mild neck contracture. There was no scoliosis or contracture of any other joints in the extremities. His extremities showed no significant muscle weakness, atrophy, or sensory disturbances. Serum CK fluctuated between 1,600 IU/mL and 3,000 IU/mL. Other routine serologic evaluations and tests for serum autoantibodies revealed no abnormalities. Using electromyography, short-duration and some unstable polyphasic motor unit potentials were detected in the right biceps brachii, but no abnormality was found in the muscles of the lower extremities. A whole-body computed tomography (CT) scan revealed low-density areas and atrophic changes in the cervical and lumbar paraspinal muscles and the left gastrocnemius (Fig. 1B, C, D).

His 48-year-old mother suffered from a first-degree atrioventricular conduction block along with paroxysmal atrial fibrillation, and was treated with warfarin. In addition, unspecified abnormal ECGs were observed when his 24-year-old twin elder sisters were screened, but no abnormalities could be detected in the workup. Periodic health examinations were advised for all three of his family members. Muscle CT examination was not performed in these probable female carriers.

The study protocol was reviewed and approved by the Institutional Review Board of Kagoshima University. The patient provided his written, informed consent to participate in this study.

Pathological studies

A skeletal muscle sample was obtained from the biceps brachii, but no skin sample was collected. Histochemical staining revealed mild variations in fiber diameter, a few degenerating or regenerating fibers, a slight increase in the

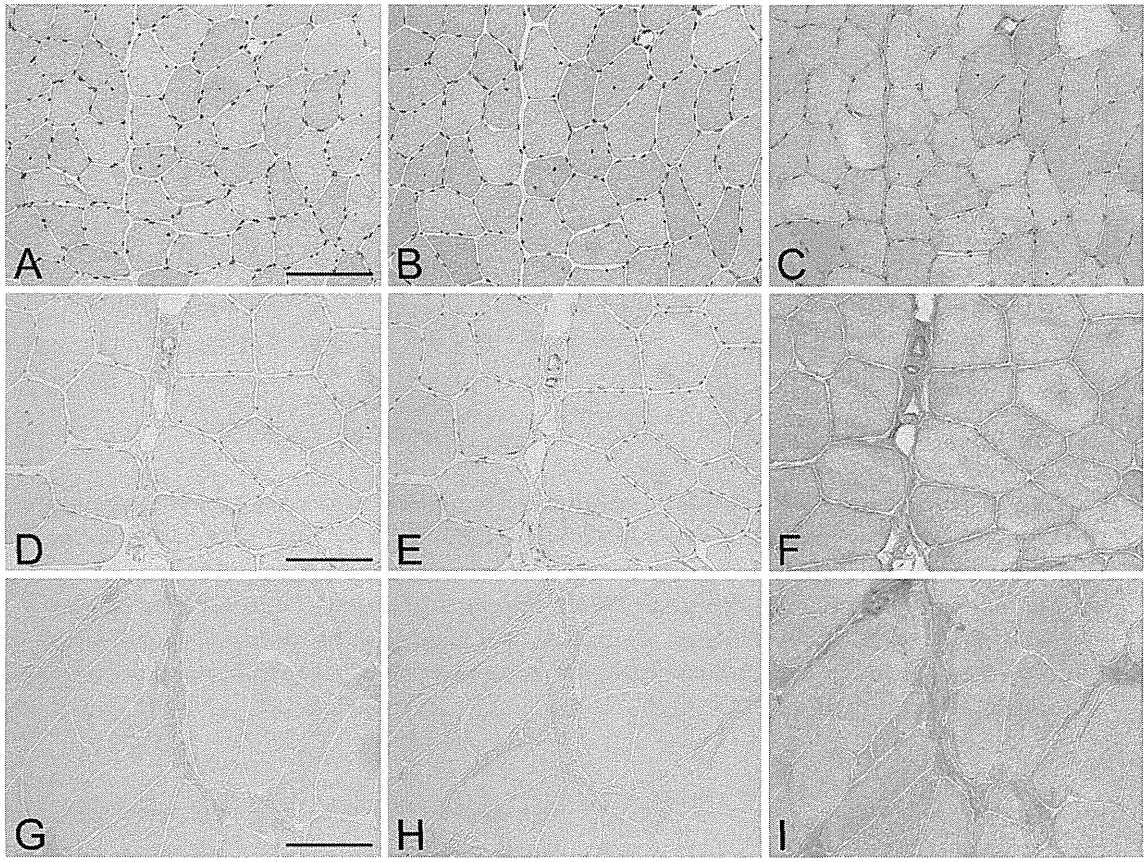

Figure 2. **Serial immunohistochemical staining with NCL-Emerin (A, D, G), H-12 (B, E, H), and C-20 (C, F, I) antibodies. A-C: Emerin was strongly expressed on the nuclei of skeletal muscle fibers in the healthy control subject. D-F: In the patient, emerin expression was significantly decreased as detected by NCL-Emerin and H-12 labeling, and it was completely absent as assessed by C-20 labeling. G-I: In the disease control, staining experiments revealed a complete absence of emerin with all three antibodies. No counterstain was used. Bar = 100 μm**

number of internal nuclei, and slight connective tissue proliferation. The number of hypertrophic fibers was increased. Immunohistochemical stains were performed manually with a 1:50 dilution of NCL-Emerin (Novocastra, Leica Microsystems, Newcastle Upon Tyne, UK), H-12 (Santa Cruz Biotechnology, Santa Cruz, USA) monoclonal antibodies for the N-terminus of emerin, and a 1:20 dilution of C-20 affinity purified polyclonal antibody for the C-terminus of emerin (Santa Cruz Biotechnology). A skeletal muscle specimen from an unrelated 39-year-old male with typical X-linked EDMD was used as a disease control. The three antibodies detected emerin expression on the nuclei of the skeletal muscle in the healthy control subject. In our patient, emerin expression was significantly decreased as detected by NCL-Emerin and H-12 labeling, and it was completely absent with C-20 labeling. In the disease control specimen, nuclear staining was absent with all three antibodies against emerin (Fig. 2). In western blot analyses using the three antibodies, we could not detect any clear bands in the patient's samples, and this was probably due to the low expression of protein or detection sensitivity of western blot (data not shown).

Genetic studies

Genomic DNA was extracted from the patient's blood lymphocytes. We were not able to obtain consent for genetic analysis from his three family members or the disease control patient. Using the Primer3 (v. 0.4.0) online program (http://frodo.wi.mit.edu/), we designed oligonucleotide primers flanking the six exons and intron-exon junctions in the *EMD* gene. After hot-start polymerase chain reaction (PCR) amplification, the products were sequenced by dye-terminator chemistry using an ABI3010 sequencer (Applied Biosystems, Foster City, USA). A splice acceptor site mutation located at the second nucleotide before exon six (c.450-2A>G) of *EMD* was identified. This created a new restriction site for AvaI. Using the forward (5'-CTCGCCCTGACT CTCTTCTG-3') and reverse (5'-CTAAGGCAGTCAGCCAG GAC-3') primers, a 533-bp PCR product covering this mutation was amplified and was divided into 385 bp and 148 bp fragments (Fig. 3A, B). This mutation was not detected in 100 Japanese control chromosomes, and we did not find the c.450-2A>G mutation in the 1,000 Genomes database that catalogs human genetic variations in 2,500 samples, including 500 East Asian (100 Japanese) samples (http://